

# Alpha Particle and Neutron-induced Soft Error Rates and Scaling Trends in SRAM

Hajime Kobayashi, Nobutaka Kawamoto, Jun Kase and Ken Shiraishi

Sony Corporation

Atsugi Tec. No.2, 4-16-1 Okata Atsugi-shi, Kanagawa, 243-0021 Japan

phone: +81-46-226-3235; fax: +81-46-226-2178; e-mail: [HajimeA.Kobayashi@jp.sony.com](mailto:HajimeA.Kobayashi@jp.sony.com)

**Abstract**—We performed underground real-time tests to obtain alpha particle-induced soft error rates ( $\alpha$ -SER) with high accuracies for SRAMs with 180 nm - 90 nm technologies and studied the scaling trend of  $\alpha$ -SERs. In order to estimate the maximum permissive rate of alpha emission from package resin, the  $\alpha$ -SER was compared to the neutron-induced soft error rate (n-SER) obtained from accelerated tests. We found that as devices are scaled down, the  $\alpha$ -SER increased while the n-SER slightly decreased, and that the  $\alpha$ -SER could be greater than the n-SER in 90 nm technology even when the ultra-low-alpha (ULA) grade, with the alpha emission rate  $< 1 \times 10^{-3} \text{ cm}^{-2}\text{h}^{-1}$ , was used for package resin. We also performed computer simulations to estimate scaling trends of both  $\alpha$ -SER and n-SER up to 45 nm technologies, and noticed that the  $\alpha$ -SER decreased from 65 nm technology while the n-SER increased from 45 nm technology due to direct ionization from the protons generated in the n + Si nuclear reaction.

**Keywords:** SER, soft error, alpha particle, neutron, SRAM, package resin

## I. INTRODUCTION

As LSI has been scaled down, the major source of terrestrial soft error in LSI has changed. Alpha particles emitted from the radioactive impurities in package resin were the major source of terrestrial soft error in the 1980's [1]. After tireless efforts to reduce the radioactive impurities, device reliability was made tolerable. In the 1990's, cosmic ray neutrons were assumed to be the major source of soft error [2-4]. However, it was pointed out from accelerated tests using a nuclear reactor that thermal neutrons could induce soft error in LSIs having a borophosphosilicate glass (BPSG) layer [5, 6]. Real-time tests furthermore showed that the thermal neutron was the major source of soft error in the actual usage condition [7]. On the other hand, it was found from underground real-time tests that alpha particle-induced soft error rates ( $\alpha$ -SER) were negligible in 180 nm SRAM [7]. The thermal neutron-induced SER also became negligible after the 180 nm process since BPSG was thereafter not used. As a result, cosmic ray neutrons with energies greater than several MeV have been considered to be the major source of terrestrial soft error, and many studies on the neutron-induced soft error have been carried out.

However,  $\alpha$ -SER should also be carefully considered to as LSI is scaled down since it increases faster than the neutron-induced soft error rate (n-SER) as voltage decreases [6, 8].

Therefore, it is very important to compare the absolute values of  $\alpha$ -SER and n-SER, and to understand their scaling trends. Accelerated tests using isotopes such as  $^{241}\text{Am}$  or  $^{232}\text{Th}$  have usually been used to obtain  $\alpha$ -SER. However, since they have less accuracy due to the difference in the energy spectra and the angular distributions of alpha particles, real-time tests are desirable to obtain the absolute value of  $\alpha$ -SER. Furthermore, real-time  $\alpha$ -SER tests should be performed underground to eliminate the cosmic ray neutron-induced soft errors.

We performed underground real-time tests to obtain  $\alpha$ -SER with high accuracy for SRAMs with 180 nm - 90 nm technologies assembled in wire-bonded structure, and compared the  $\alpha$ -SER to the n-SER obtained from accelerated tests in order to estimate the maximum permissive rate of alpha emission from package resin. We also investigated the alpha emission rates of numerous package resins bought from various vendors. Furthermore, we performed computer simulations to estimate the scaling trends of both the  $\alpha$ -SER and the n-SER up to 45 nm technologies.

## II. EXPERIMENTS

The underground real-time tests were performed at the Oto Cosmo Observatory of the Research Center for Nuclear Physics at Osaka University (Fig. 1). This facility is at a depth of 470 m and shielded from cosmic ray neutrons which are reduced to  $< 1/100$ . Several hundred SRAMs with 180 nm, 130 nm and 90 nm technologies were tested for several months. Table I summarizes the underground  $\alpha$ -SER tests. The same

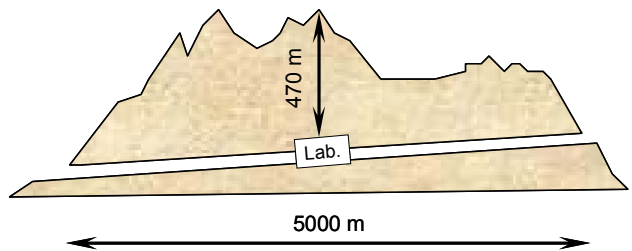


Fig. 1. Oto Cosmo Observatory of the Research Center for Nuclear Physics at Osaka University. The laboratory is located at the center of a tunnel at a depth of 470 m and shielded from cosmic ray neutrons which are reduced to  $< 1/100$ .

TABLE I. SUMMARY OF THE UNDERGROUND REAL-TIME  $\alpha$ -SER TESTS.  
PACKAGE RESINS WITH HIGH ALPHA EMISSION RATES WERE USED  
INTENTIONALLY FOR 130 NM AND 90 NM DEVICES TO ACCELERATE TESTS  
FOR BETTER STATISTICAL ACCURACIES.

Technology (nm)	180	130	90
Duration (h)	4194	4854	5059
$^{238}\text{U}$ concentration (ppb)	0.25	17	8.7
$^{232}\text{Th}$ concentration (ppb)	0.22	7.3	17
Alpha emission rate from package resin ( $\text{cm}^{-2}\text{h}^{-1}$ )	$1.7 \times 10^{-4}$	$1.0 \times 10^{-2}$	$7.6 \times 10^{-3}$
Acceleration factor	1	59	45
No. of errors	1	142	244
Statistical error ( $\sigma$ )	100%	8.3%	6.4%

package resin as used in the actual device was used for 180 nm SRAM, whereas in order to obtain better statistical accuracies package resins with high alpha emission rates were used intentionally for 130 nm and 90 nm SRAMs to accelerate tests. This was a kind of accelerated test in real-time tests, and the acceleration factors of 130 nm and 90 nm SRAM to 180 nm SRAM were 59 and 45, respectively. The alpha emission rate can be measured directly by means of radiation detectors such as a proportional counter. The detection limit in such direct detection methods, however, is approximately  $1 \times 10^{-3} \text{ cm}^{-2}\text{h}^{-1}$  at best, and was not sufficient for our purpose. Therefore, we estimated the alpha emission rates by using concentrations of  $^{238}\text{U}$  and  $^{232}\text{Th}$  measured by inductively coupled plasma mass spectrometer (ICP-MS). The calculation method is shown in the appendix. The detection limit in this method was approximately  $3 \times 10^{-5} \text{ cm}^{-2}\text{h}^{-1}$ . In more than 4000 hours for the test on 180 nm SRAM, we had only one error. This indicates that any other errors except radiation-induced soft errors, such as a tester failure, were negligible.

Accelerated tests for n-SER were performed using the

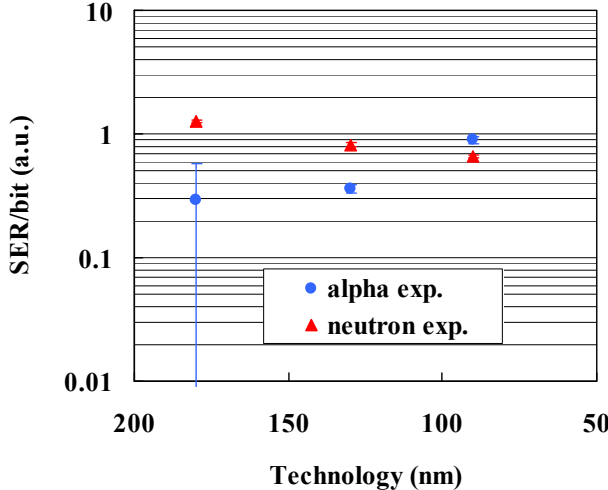


Fig. 2. Results of the underground real-time  $\alpha$ -SER tests and the accelerated n-SER tests. The  $\alpha$ -SERs were normalized to the case when the alpha emission rate was  $1 \times 10^{-3} \text{ cm}^{-2}\text{h}^{-1}$ .

WNR facility at Los Alamos National Laboratory, where an intense neutron beam with a similar energy spectrum to terrestrial cosmic neutrons is available [9]. The typical neutron flux was  $9.3 \times 10^5 \text{ n/cm}^2/\text{sec}$ , approximately  $2.4 \times 10^8$  times greater than that on ground.

Fig. 2 shows the results of the underground real-time  $\alpha$ -SER tests and the accelerated n-SER tests. No multiple-cell upset (MCU) was observed in the  $\alpha$ -SER tests and the fraction of MCU was approximately 6 % of all soft errors in the n-SER tests. The  $\alpha$ -SERs were normalized to the case when the alpha emission rate was  $1 \times 10^{-3} \text{ cm}^{-2}\text{h}^{-1}$ . The  $\alpha$ -SER increased as the devices were scaled down while the n-SER slightly decreased. The  $\alpha$ -SER became greater than the n-SER in 90 nm technology when the alpha emission rate was  $1 \times 10^{-3} \text{ cm}^{-2}\text{h}^{-1}$ .

Table II shows the alpha emission categories of package resin [10]. We investigated the alpha emission rates of numerous package resins of various vendors. The results are shown in Fig. 3. Symbols of A-1, A-2 and A-3, for example, indicated different samples of the different part number of the same vendor A. We performed ICP-MS measurements for more than two samples of the same part number, and found that the sample-to-sample variation was less than 10 %. The alpha emission rates were widely distributed from  $2 \times 10^{-4}$  to  $1 \times 10^{-3} \text{ cm}^{-2}\text{h}^{-1}$  in the ultra-low-alpha (ULA) grade. If the alpha

TABLE II. ALPHA EMISSION CATEGORIES OF PACKAGE RESIN [10].

Alpha emission categories ( $\text{cm}^{-2}\text{h}^{-1}$ )	
Standard	$10 - 0.01$
Low-alpha (LA)	$< 1 \times 10^{-2}$
Ultra-low-alpha (ULA)	$< 1 \times 10^{-3}$
Hyper-low-alpha (HLA)	$< 5 \times 10^{-4}$

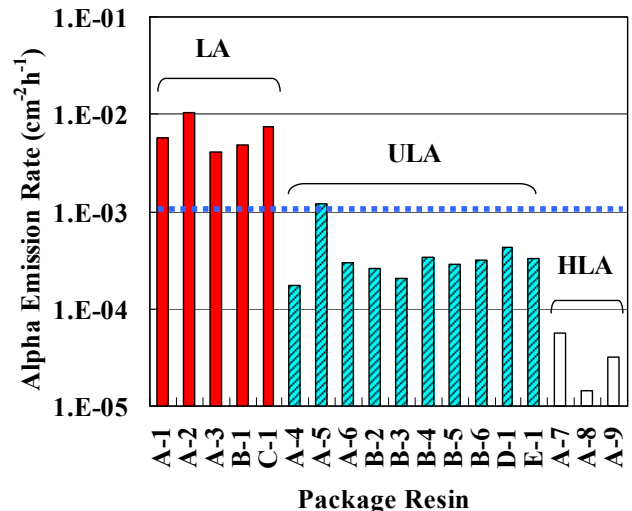


Fig. 3. Summary of the alpha emission rates of numerous package resins from various vendors (A-E). A dotted line is the guaranteed value of the ULA grade.

emission rate was the highest among the ULA grade, the  $\alpha$ -SER would be greater than the n-SER in 90 nm technology even when the ULA grade was used for package resin. Therefore, it is important to evaluate the alpha emission rate in the selection of package resin, and to use the ULA grade with an especially low alpha emission rate or the HLA grade in order to make the  $\alpha$ -SER lower than the n-SER.

### III. SIMULATION AND SCALING TRENDS

We studied the scaling trends of both the  $\alpha$ -SER and the n-SER up to 45 nm technologies using a SER simulator which we have developed. The SER simulator incorporates the Particle and Heavy Ion Transport code System (PHITS), which was developed by the Japan Atomic Energy Research Institute (JAERI), as a nuclear data base [11]. PHITS simulates nuclear reactions between incident particles and target nuclei by means of the Monte Carlo method, and also calculates deposited energy of each charged particle generated in the nuclear reactions.

In the  $\alpha$ -SER calculation, alpha particles were generated in a package resin, and then were transported in the package resin, dielectric layer and Si substrate. Radio isotopes in the uranium and the thorium decay chains contained in the package resin were assumed to be the sources of the alpha particles. Deposited energy in the Si substrate was calculated and 3-D distributions of the electric charge were obtained. In the n-SER calculation, all nuclear reactions of neutrons with the Si nucleus and O nucleus, which were contained in the Si substrate and package resin, were considered. 3-D distributions of the electric charge were obtained from deposited energy of charged particles generated in the nuclear reactions. The neutron flux on the ground was extracted from the JEDEC standard [12]. A soft error was counted when the total electric charge generated in a sensitive volume around a sensitive node exceeded the critical charge ( $Q_c$ ). The sensitive volume was the product of the sensitive area by the sensitive depth. The sensitive area was the drain area plus the depletion area, and the sensitive depth was assumed to be the funneling length. We considered only the prompt charge collection by the funneling and neglected diffusion. The funneling length was calculated using an empirical model [13]. This model defined an elliptic function as the end point of the funneling.  $Q_c$  was obtained by SPICE simulation. Device parameters used in the simulation are summarized in Table III.

The simulation results of the  $\alpha$ -SER against  $Q_c$  are shown

TABLE III. DEVICE PARAMETERS USED IN THE SER SIMULATION.

Technology (nm)	180	130	90	65	45
$V_{dd}$ (V)	1.7	1.4	1.1	1.2	1.0
$Q_c$ (fC)	6.70	3.30	1.70	0.76	0.37
Cell area (a.u.)	1.00	0.49	0.30	0.21	0.16
Thickness of dielectric layer (a.u.)	1.00	0.89	0.83	0.78	0.74

in Fig. 4-(a). The standard operation points for each device are indicated by the black circles. As technology is scaled down, SER varies mainly by the following two effects; (i) the increase effect due to the increasing upset probability with decreasing  $Q_c$ , (ii) the decrease effect due to the decreasing sensitive volume. The increase effect is that each line in Fig. 4-(a) increases as  $Q_c$  decreases. The decrease effect is that the SER decreases as device size decreases at the same  $Q_c$ . Fig. 4-(a) shows that the  $\alpha$ -SER increases up to 90 nm technology since the increase effect is greater than the decrease effect. The upset probability of each device, however, is saturated to be 100 % in the small  $Q_c$  region as all the incident alpha particles induce soft errors. In this region, the  $\alpha$ -SER is simply proportional to the product of the alpha particle flux with the sensitive area of the device. Therefore, the increase effect vanishes, and the  $\alpha$ -SER starts to decrease. Fig. 4-(a) indicates that the decrease will take place from 65 nm technology.

The simulation results of n-SER against  $Q_c$  are summarized in Fig. 4-(b). The n-SER slightly decreases up to 65 nm

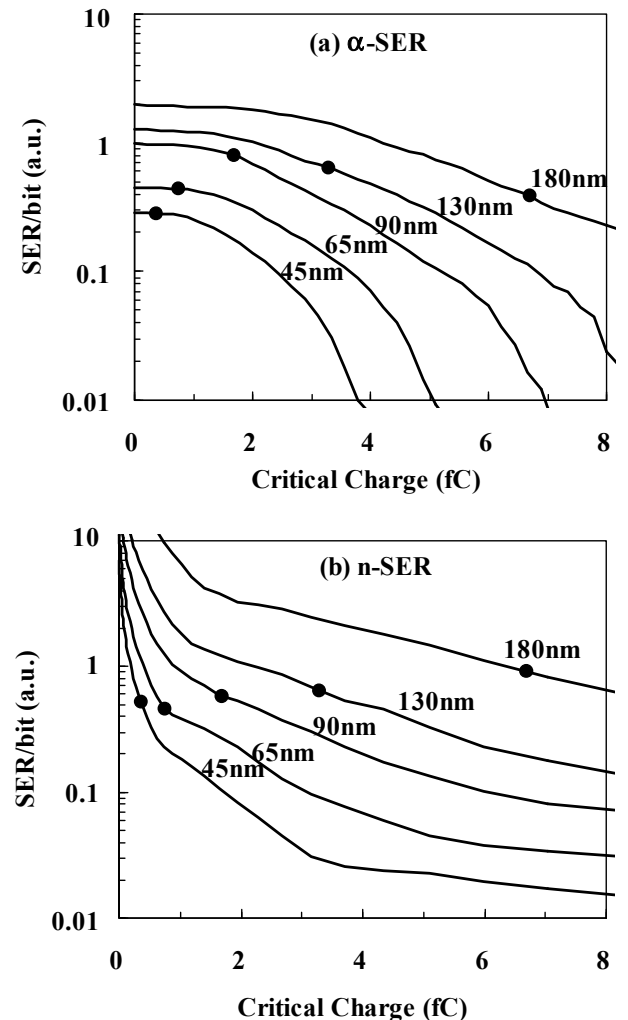


Fig. 4. Simulation results of (a)  $\alpha$ -SER and (b) n-SER against critical charge. The black circles indicate the standard operation points for each device.

technology since the decrease effect is greater than the increase effect. However, it slightly increases in 45 nm technology since it is in the sharp increase region at  $Q_c < 0.6$  fC. Fig. 5 shows the comparison of the simulation and the experimental results.

Fig. 6 shows the contributions of various particles generated in the nuclear reactions of neutron and Si nuclei to the n-SER of 45 nm SRAM. It is clearly seen that the major source of soft error varies with  $Q_c$ . Heavy nuclei such as Si, Al and Mg are crucial at  $Q_c > 3$  fC. Alpha particles become dominant at  $0.6 \text{ fC} < Q_c < 3$  fC, and protons become the major source at  $Q_c < 0.6$  fC. The sharp increase of n-SER at  $Q_c < 0.6$  fC in Fig. 4- (b) was found to be due to the proton contribution. This can be explained intuitively as follows. Figs. 7 and 8 show linear energy transfer (LET) and the ranges of the proton and alpha particle in Si, respectively [14].

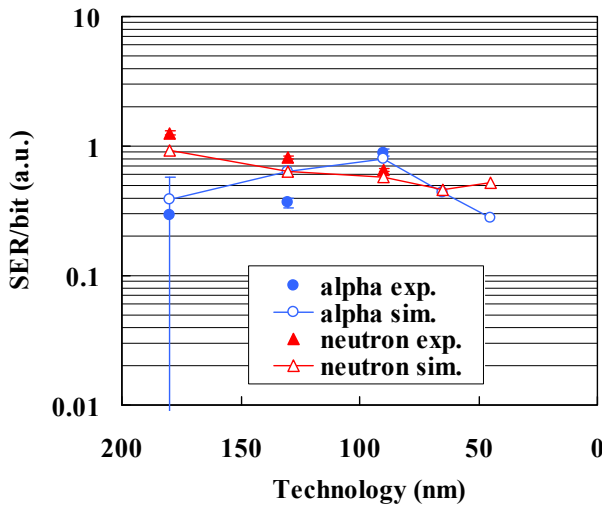


Fig. 5. Comparison of the simulation and the experimental results.

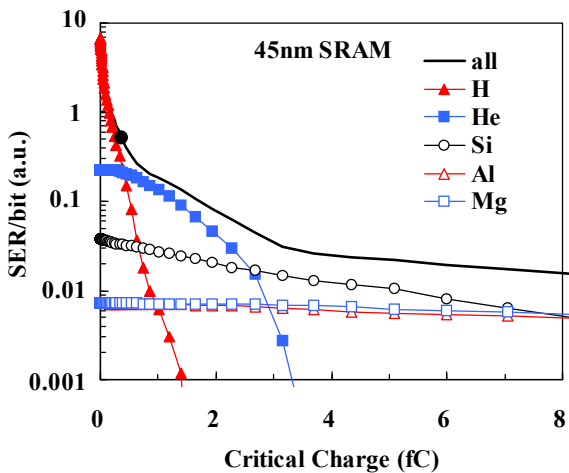


Fig. 6. Contributions from various particles generated in the nuclear reactions of neutron and Si nuclei to the n-SER of 45 nm SRAM. The black circle on the "all" line indicates the standard operation point of the device.

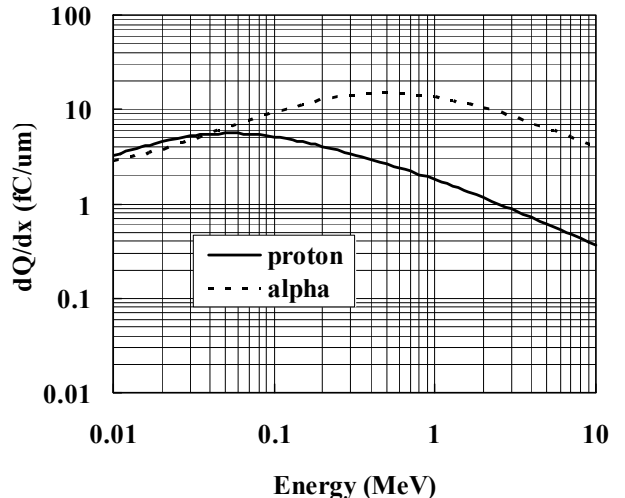


Fig. 7. LET of proton and alpha particle [14]. The unit of LET was converted into electric charge per distance generated in Si.

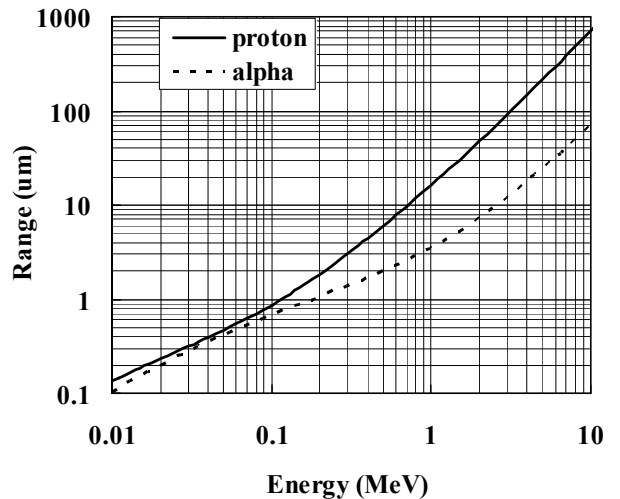


Fig. 8. Range of proton and alpha particle in Si [14].

The unit of LET was converted into electric charge generated in Si per distance. The LET of proton has the maximum value of approximately 5 fC/ $\mu\text{m}$  at energy of 50 keV. The range of proton at this energy is 0.5  $\mu\text{m}$ , i.e. the deposited energy is approximately 2 fC. Since the sensitive depth and  $Q_c$  of 45 nm SRAM are approximately 0.3  $\mu\text{m}$  and 0.4 fC, respectively, sufficient electric charge to induce soft errors can be generated by such low energy protons. The average energy of protons generated in the nuclear reaction between cosmic ray neutrons and Si nuclei is approximately 5 MeV. The range of proton in this energy region is much greater than that of alpha particle as shown in Fig. 8, for example, the range of alpha particle is 24  $\mu\text{m}$  at energy of 5 MeV while that of proton is 200  $\mu\text{m}$  at the same energy. It suggests that protons generated in a larger volume can contribute soft errors compared to alpha particles, and that a large quantity of low energy protons (i.e. high LET protons), which have lost their energies after traveling long

distances, can pass through a sensitive volume in the device. Therefore, as  $Q_c$  decreases, soft errors can be induced by direct ionization from such low energy protons. This is consistent with the recent experimental result that a sharp rise in the upset cross section was observed in the low energy proton test below 1 MeV, which was attributed to upsets caused by direct ionization from the low energy proton [15].

In simulation, it is essential to make the nuclear reaction region large enough. The nuclear reaction region was approximately  $100 \mu\text{m} \times 100 \mu\text{m} \times 100 \mu\text{m}$  in previous simulation works for devices with relatively large  $Q_c$  where the proton contribution was negligible. In this work, we enlarged the nuclear reaction region to  $1 \text{ mm} \times 1 \text{ mm} \times 1 \text{ mm}$  to take the proton contribution into account. Since the n-SER of 45 nm SRAM can be varied considerably by slight differences in device structures and/or operation voltages due to the proton contribution, much attention should be paid to the design, process and operation of the device.

#### IV. CONCLUSIONS

From the underground real-time  $\alpha$ -SER tests and the neutron accelerated tests, we found that the  $\alpha$ -SER increased up to 90 nm technologies and that the  $\alpha$ -SER can be greater than the n-SER even when the ULA grade was used for package resin. We investigated the alpha emission rate of numerous package resins, and found that they were widely distributed by a factor of 5 in the ULA grade. It is important to evaluate the alpha emission rate in the selection of package resin. Simulation results suggested that the  $\alpha$ -SER would decrease from 65 nm technology. In contrast, the n-SER slightly decreased up to 65 nm technologies and increased from 45 nm technologies due to direct ionization from the protons generated in the  $n + Si$  nuclear reaction.

#### APPENDIX

##### *Calculation method to estimate alpha emission rate from impurity concentrations.*

We derived an equation using Monte Carlo method to estimate the alpha emission rate from concentrations of  $^{238}\text{U}$  and  $^{232}\text{Th}$  in package resin in the following way.

- All decays which emit alpha particles in the  $^{238}\text{U}$  and  $^{232}\text{Th}$  decay chains were considered. We assumed that the  $^{238}\text{U}$  and  $^{232}\text{Th}$  decay chains were in secular equilibrium as described in the JEDEC standard [12]. The energy spectrum of alpha particles is shown in Fig. 9 to the case when  $^{238}\text{U}$  and  $^{232}\text{Th}$  are present in equal amounts. Angular distribution of alpha particles was considered to be isotropic.
- The alpha particles were generated along the center line in the package resin of  $100 \mu\text{m-thick} \times 200 \mu\text{m} \times 200 \mu\text{m}$  with a uniform probability. Transportation of the alpha particles was performed by means of PHITS. We assumed that the package resin was made of 90 wt% of  $\text{SiO}_2$  (filler) and 10 wt% of epoxy resin. The density of the package resin was  $2.0 \text{ g/cm}^3$ . We treated the package resin as homogeneous since the filler consisted of small particles

with various diameters forming a nearly close-packed structure. Fig. 10 shows an example of the PHITS calculation.

- The probabilities of alpha particles being emitted from the package resin were obtained for the  $^{238}\text{U}$  and  $^{232}\text{Th}$  decay chains, respectively. We obtained the following relationship between the concentrations of  $^{238}\text{U}$  ( $= C_U$ ),  $^{232}\text{Th}$  ( $= C_{Th}$ ) and the alpha emission rate ( $= AER$ ).

$$AER [\text{cm}^{-2}\text{h}^{-1}]$$

$$= 5.4 \times 10^{-4} \times C_U [\text{ppb}] + 1.7 \times 10^{-4} \times C_{Th} [\text{ppb}]$$

The detection limit for the concentration measured by ICP-MS was approximately 0.05 ppb for both  $^{238}\text{U}$  and  $^{232}\text{Th}$ . Therefore, the detection limit for the alpha emission rate in this method was approximately  $3 \times 10^{-5} \text{ cm}^{-2}\text{h}^{-1}$ . Fig. 11 shows the energy spectrum of the alpha particles emitted from the package resin to the case when  $^{238}\text{U}$  and  $^{232}\text{Th}$  are present in equal amounts.

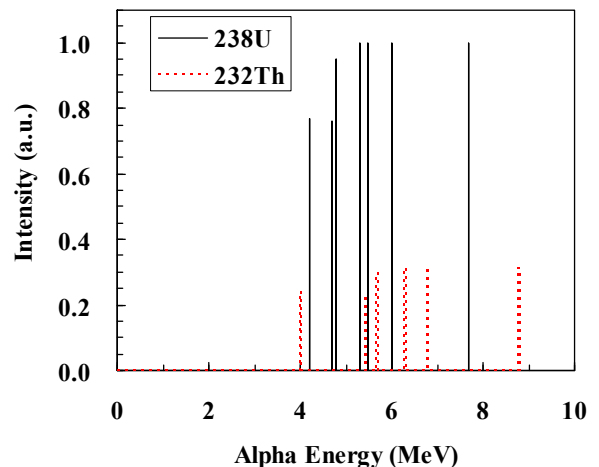


Fig. 9. Energy spectrum of alpha particles from  $^{238}\text{U}$  and  $^{232}\text{Th}$  decay chains.

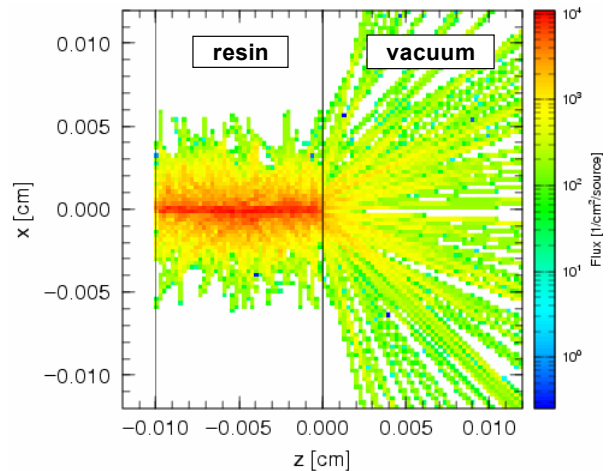


Fig. 10. Example of PHITS calculation for transportation of alpha particles.

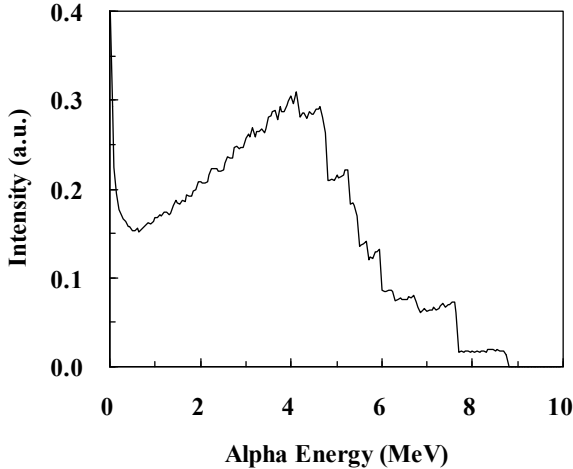


Fig. 11. Energy spectrum of the alpha particles emitted from the package resin.

#### ACKNOWLEDGMENT

The authors would like to thank Kichiji Hatanaka, Mitsuhiro Fukuda and Keiji Takahisa of Osaka University for their support in performing underground tests at the Oto Cosmo Observatory. We gratefully thank Koji Niita of the Research Organization for Information Science and Technology, Yukio Sakamoto and Yosuke Iwamoto of the Japan Atomic Energy Agency for their support in using PHITS code. The authors would also like to thank Bruce Takala and Steve Wender of the Los Alamos National Laboratory for providing the neutron beams used in this work.

#### REFERENCES

- [1] T. C. May and M. H. Woods, "A new physical mechanism for soft errors in dynamic memories", in *Proc. Int. Reliab. Phys. Symp. (IRPS)*, 16, pp. 33–40, 1978.
- [2] J. F. Ziegler and W. A. Lanford, "Effect of cosmic rays on computer memories", *Science*, vol. 206, no. 4420, pp. 776-788, 1979.
- [3] A. Taber and E. Normand, "Single event upset in avionics", *IEEE Trans. Nucl. Sci.*, vol. 40, no.2, pp.120-126, 1993.
- [4] J. F. Ziegler et al., "IBM experiments in soft fails in computer electronics (1978-1994)", *IBM J. Res. Develop.*, vol. 40, no.1, pp.3-18, 1996.
- [5] R. C. Baumann, T. Hossain, S. Murata and H. Kitagawa, "Boron compounds as a dominant source of alpha particles in semiconductor devices", in *Proc. Int. Reliab. Phys. Symp. (IRPS)*, pp.297-302, 1995.
- [6] R. C. Baumann and E. B. Smith, "Neutron-induced 10B fission as a major source of soft errors in high density SRAMs", *Microelectro. Reliab.*, vol. 41, pp. 211-218, 2001.
- [7] H. Kobayashi, K. Shiraishi, H. Tsuchiya, M. Motoyoshi, H. Usuki, Y. Nagai, K. Takahisa, T. Yoshiie, Y. Sakurai and T. Ishizaki, "Soft errors in SRAM devices induced by high energy neutrons, thermal neutrons and alpha particles", in *Int. Electron Devices Meeting (IEDM) Tech. Dig.*, pp. 337-340, 2002.
- [8] F. Wrobel, J. Gasiot and F. Saigne, "Hafnium and Uranium Contributions to Soft Error Rate at Ground Level", *IEEE Trans. Nucl. Sci.*, vol. 55, no. 6, pp.3141-3145, 2008.
- [9] P. W. Lisowski, C. D. Bowman, G. J. Russell and S. A. Wender, "The Los Alamos National Laboratory spallation neutron sources", *Nucl. Sci. Eng.*, vol. 106, pp. 208-218, 1990.
- [10] X. Zhu, "Logic SER characterization", Tutorial, *Int. Reliab. Phys. Symp. (IRPS)*, 2008.
- [11] <http://www-conf.kek.jp/geant4/1213/koji.niita.pdf>.
- [12] JEDEC standard, "Measurement and reporting of alpha particles and terrestrial cosmic ray-induced soft errors in semiconductor devices", *JESD89A*, 2006.
- [13] S. Satoh, R. Sudo, H. Tashiro, N. Higaki and N. Nakayama, "CMOS-SRAM soft-error simulation system", in *Proc. Int. Reliab. Phys. Symp. (IRPS)*, pp. 339-343, 1994.
- [14] J. F. Ziegler, SRIM 2003.
- [15] D. F. Heidel, P. W. Marshall, K. A. LaBel, J. R. Schwank, K. P. Rodbell, M. C. Hakey, M. D. Berg, P. E. Dodd, M. R. Friendlich, A. D. Phan, C. M. Seidleck, M. R. Shaneyfelt and M. A. Xapsos, "Low Energy Proton Single-Event-Upset Test Results on 65 nm SOI SRAM", *IEEE Trans. Nucl. Sci.*, vol. 55, no. 6, pp.3394-3400, 2008.